Continuum Mech. Thermodyn.
https://doi.org/10.1007/s00161-020-00921-0

ORIGINAL ARTICLE

**O. S. Loboda · E. A. Podolskaya · D. V. Tsvetkov · A. M. Krivtsov**

# On the fundamental solution of the heat transfer problem in one-dimensional harmonic crystals

Received: 28 March 2020 / Accepted: 21 August 2020


**Abstract** The work is devoted to the description of unsteady thermal processes in low-dimensional structures. To obtain the relationship between the microscopic and macroscopic descriptions of solids, it is necessary to understand the heat transfer mechanism at the micro-level. At the latter, in contrast to the macro-level, analytical, numerical, and experimental studies demonstrate significant deviations from the Fourier's law. The paper bases on the ballistic heat transfer model, according to which the heat is carried by the thermal waves. This effect can be applied, for example, to signal transmission and heat removal problems. The influence of non-nearest neighbors on processes in discrete media, as well as processes in polyatomic lattices, is investigated. To describe the evolution of the initial thermal perturbation, the dispersion characteristics and group velocities in one-dimensional crystal are analyzed for (i) a diatomic chain with variable masses or stiffnesses and for (ii) a monatomic chain with regard for interaction with second neighbors. A fundamental solution to the heat distribution problem for the corresponding crystal models is obtained and investigated. The fundamental solution allows to obtain a description of waves traveling from a point source, and can serve as the basis for constructing all other solutions. In both cases, the solution consists of two thermal fronts moving one after another with different speeds and intensities. Quantitative estimates of the intensity of the thermal wave front are given, and the dynamics of changes in the velocities and intensities of the waves depending on the parameters of the problem is analyzed. Thus, a simple method for estimating the wavefronts intensity is proposed and tested on two models. These results can be used to identify and analyze those parts of the wave processes that are of interest in terms of interpretation of the effects observed in the experiments.

**Keywords** Thermal processes · Kinetic temperature · One-dimensional crystal · Fundamental solution · Ballistic heat transfer · Group velocity

## 1 Introduction

At the macroscopic level, the heat propagation in the majority of the materials is described by the Fourier's law, which assumes a linear relationship between the heat flux and the temperature gradient with a proportionality coefficient, defined as the thermal conductivity coefficient. However, at small temporal and spatial scales,

Communicated by Andreas Öchsner.

This work was supported by the Government of the Russian Federation (state assignment 0784-2020-0027).

O. S. Loboda (✉) · E. A. Podolskaya · D. V. Tsvetkov · A. M. Krivtsov
Peter the Great St. Petersburg Polytechnic University, Saint Petersburg, Russian Federation
E-mail: loboda_o@mail.ru

O. S. Loboda · E. A. Podolskaya · A. M. Krivtsov
Institute for Problems in Mechanical Engineering RAS, Saint Petersburg, Russian Federation

Published online: 06 September 2020

there are noticeable deviations from the Fourier's law [1,2]. To understand the heat transfer mechanism at the micro-level, it is essential to obtain a connection between the micro- and macroscopic descriptions of processes in solids. One of the powerful tools for studying mechanical processes at the micro- and macro-levels is the approach based on crystal lattice dynamics [3–14]. It is known [15–17], that in simple discrete systems, such as a one-dimensional harmonic crystal, the heat propagation does not obey the Fourier's law. The main reason is that ballistic heat transfer dominates at the micro-level, in contrast to the macro-level, where diffusion (Fourier's) thermal conductivity prevails. The anomalies associated with ballistic heat transfer are most noticeable for the harmonic crystal model.

Currently, the problem of unsteady thermal processes at the molecular level has an exact analytical solution only for a limited class of systems. Significant progress has been achieved for harmonic crystals [17–24]. The analytical approach to the description of ballistic heat transfer in harmonic lattices is presented in [25–29], where the kinetic temperature is introduced as a value proportional to the sum of kinetic energies of particles in a unit cell. For the one-dimensional non-quantum case, the macroscopic heat equation and the corresponding anomalous heat conductivity law, an alternative to the Fourier's law, are obtained. This law predicts the finite velocity of heat fronts and the independence of the heat flux from the crystal length. Using correlation analysis, the initial stochastic problem for individual particles is reduced to a deterministic problem for the crystal statistical characteristics. A generalization of this approach to heat distribution in multidimensional systems is presented in [18,23,24,29]. Note that the temperature definition used in this series of works is not related to specific wavelengths: the whole spectrum of frequencies contributes to a kinetic temperature.

An important issue is the study of the influence of non-nearest neighbors on processes in discrete media, as well as on processes in polyatomic lattices. The dynamic features of discrete systems with additional non-nearest neighbor interactions are studied in [30–32]. The analysis of dispersion characteristics and group velocities for a diatomic chain with variable masses or stiffnesses and a monatomic chain taking into account interaction with second neighbors is carried out in [33,34], respectively. It is shown that in such systems, two thermal waves are generated, which propagate with different velocities and intensities. Initial conditions in the form of a Heaviside function and a rectangular pulse are considered, and numerical solutions describing the evolution of the initial thermal perturbation are obtained. In these works, only velocities of thermal wave propagation are determined.

To sum everything up, at the micro-level the heat is carried by the thermal waves. This is a novel effect of high significance, as it can be applied to signal transmission and heat removal, e.g., in nano- and micro-electromechanical systems [20]. The speed of these waves is determined quite easily [18,26,33,34]. However, their amplitudes also play an important part, and they can vary dramatically. For example, consider a wave traveling with a relatively high speed, so this wave seems to be the means of fast signal transfer. But, as shown below, it may turn out to have such a small amplitude that the share of energy carried by this wave is negligible, and its practical value vanishes. Thus, a simple method to determine the wavefronts intensities is required.

This work is devoted to the study of the thermal wavefront intensity. In Sect. 3, we propose an analytical approach that allows to extract its the main part. Namely, in the framework of the previously developed approach to the ballistic heat conduction description, a fundamental solution to the problem of heat transfer in dynamic systems with various properties is constructed and analyzed: in Sect. 4, for a diatomic chain with variable masses or stiffnesses, and in Sect. 6 for a monatomic chain, taking into account interaction with second neighbors. The fundamental solution allows to describe waves propagating from a point source and can serve as a basis for all other solutions. Quantitative estimates of the thermal wavefront intensity are presented; the dynamics of changes in velocities and intensity coefficients of waves depending on the parameters of the problem is revealed.

## 2 Statement of the problem

It is shown in [18] that the evolution of the initial temperature field $T_0(x)$ in a monatomic chain is described by the formula

$$T(x,t) = T_F + T_S, \quad T_F = \frac{T_0(x)}{4\pi}\int_{-\pi}^{\pi} \cos(2\Omega t)\mathrm{d}\,(Ka)\,,$$
$$T_S = \frac{1}{8\pi}\int_{-\pi}^{\pi}\Big(T_0\big(x + c_g\,(Ka)\,t\big) + T_0\big(x - c_g\,(Ka)\,t\big)\Big)\mathrm{d}\,(Ka)\,, \tag{1}$$

where $K$ is wavenumber, $a$ is the distance between the neighboring particles, $\Omega$ is frequency, $c_g$ is the group velocity of waves in a chain. That is, at large times, when fast processes $T_F$ vanish, the temperature field $T_S$ is a superposition of waves moving with group velocities $c_g$, and has the form of the initial heat distribution $T_0$. Equation (1) is obtained as the initial stochastic problem is reduced to the deterministic one for the statistical characteristics of the crystal using correlation analysis; it reflects the ballistic nature of heat transfer.

We restrict ourselves further to the consideration of the heat transfer problem, i.e., $T(x,t) \approx T_S$. For a chain consisting of atoms of several types, formula (1) can be rewritten [31,33]:

$$T(x,t) \approx T_S = \frac{1}{8\pi N} \int_{-\pi}^{\pi} \sum_{j=1}^{N} \Big( T_0\big(x + c_{g_j}(Ka)\,t\big) + T_0\big(x - c_{g_j}(Ka)\,t\big) \Big) \mathrm{d}(Ka)\,, \tag{2}$$

where $N$ is the number of types of atoms, $a$ the distance between the unit cells, $c_{g_j}$ are the respective group velocities ($j = 1 \dots N$). The calculation of temperature using equation (2) requires knowledge of the group velocity that is determined by the particular problem..

## 3 Algorithm for constructing an approximate fundamental solution

In this section, we build an approximate fundamental solution to the heat transfer problem. Let the initial thermal perturbation be given in the form of a delta function

$$T_0(x) = T_0 \delta(x), \tag{3}$$

where $T_0$ is the amplitude of the initial thermal perturbation. Then, after the kinetic and potential energies equilibrate, formula (2) takes the form

$$T(x,t) = \frac{T_0}{8\pi N} \int_{-\pi}^{\pi} \sum_{j=1}^{N} \Big( \delta\big(x + c_{g_j}(Ka)\,t\big) + \delta\big(x - c_{g_j}(Ka)\,t\big) \Big) \mathrm{d}(Ka)\,. \tag{4}$$

Given the property of the delta function $\delta(\lambda x) = \dfrac{\delta(x)}{|\lambda|}$, we obtain

$$T = \frac{T_0}{8\pi N t} \int_{-\pi}^{\pi} \sum_{j=1}^{N} \left( \delta\left(\frac{x}{t} + c_{g_j}(Ka)\right) + \delta\left(\frac{x}{t} - c_{g_j}(Ka)\right) \right) \mathrm{d}(Ka)\,. \tag{5}$$

Besides, the integral of the delta function can be represented as [36]

$$\int \delta\big(f(z)\big) = \sum_j \frac{\delta(z - z_j)}{|f'(z_j)|}, \quad f(z_j) = 0, \tag{6}$$

where the summation is carried out over the real roots of the equation $f(z) = 0$, so that formula (5) yields to

$$T = \frac{T_0}{4\pi N t} \sum_j \sum_i \frac{1}{|c'_{g_j}(K_i a)|}, \tag{7}$$

where $K_i$ are the solutions to the equations

$$|c_{g_j}(K_i a)| = \frac{|x|}{t} \tag{8}$$

In order to quantify the intensity of the wavefront, we construct an approximation of function (7) near its singular points, i.e., the roots of the denominator. For a monatomic chain, the solution has a simple form. Indeed, let us introduce the variable $\zeta = x/t$ and consider a function

$$\Phi = \frac{1}{\xi}, \quad \xi = |c'(Ka)|, \quad |c(Ka)| = |\zeta|. \tag{9}$$

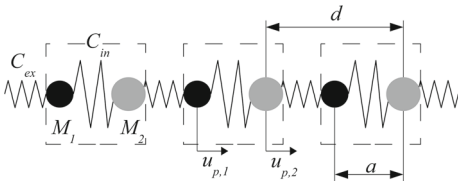


**Fig. 1** Model of a one-dimensional diatomic harmonic crystal (dotted lines indicate unit cells)

At singular points, given that the front propagates with a maximum group velocity, we have

$$\xi = 0 \quad \Rightarrow \quad K = K_*, \quad \zeta = \zeta_*, \quad c'(K_*a) = 0, \quad c''(K_*a) < 0 \tag{10}$$

and in the vicinity of the singular points

$$\xi \neq 0, \quad Ka = K_*a + Z \tag{11}$$

We restrict ourselves to the positive coordinate $x$ and expand the group velocity and its derivative in a Taylor series in a neighborhood of $K_*a$

$$\begin{aligned} \xi &= |c'(K_*a + Z)| \approx \left|c'(K_*a) + c''(K_*a)Z\right| \\ \zeta &= |c(K_*a + Z)| \approx \left|c(K_*a) + c'(K_*a)Z + \frac{1}{2}c''(K_*a)Z^2\right|, \end{aligned} \tag{12}$$

which, taking (9) into account, is rewritten in the form

$$\xi = |c''(K_*a)||Z|, \quad \zeta = \zeta_* - \frac{1}{2}|c''(K_*a)|Z^2 \quad \Rightarrow \quad |Z| = \sqrt{\frac{2(\zeta_* - \zeta)}{|c''(K_*a)|}}, \tag{13}$$

then in the end

$$\Phi = \frac{1}{\xi} = \frac{A}{\sqrt{\zeta_* - \zeta}}, \quad A = \frac{1}{\sqrt{2|c''(K_*a)|}}, \tag{14}$$

where $A$ is the coefficient which characterizes the wavefront intensity; hereinafter we will refer to it as the intensity coefficient.

In the following parts of the work, such an approximation will be constructed for two systems: a diatomic chain with variable masses or stiffnesses and a monatomic chain taking into account the interaction with distant neighbors.

## 4 Example (i): A chain with variable masses/stiffnesses

Consider a one-dimensional diatomic harmonic crystal with variable masses or stiffnesses Fig. 1 [33].

The equations of lattice dynamics have the form

$$\begin{aligned} M_1\ddot{u}_{p,1} &= C_{\text{ex}}\left(u_{p-1,2} - u_{p,1}\right) + C_{\text{in}}\left(u_{p,2} - u_{p,1}\right), \\ M_2\ddot{u}_{p,2} &= C_{\text{ex}}\left(u_{p+1,1} - u_{p,2}\right) + C_{\text{in}}\left(u_{p,1} - u_{p,2}\right), \end{aligned} \tag{15}$$

Here, $u_{p,1}$,$u_{p,2}$ are the displacements of the left particle of mass $M_1$ and of the right particle of mass $M_2$ in a unit cell number $p$, $C_{\text{in}}$ and $C_{\text{ex}}$ are the bonds' stiffnesses between particles in the cell and between cells, respectively. Following [37], we introduce the equilibrium distances between particles: $a$ inside the cell, $(d - a)$ between the cells; thus, the "length" of the unit cell is equal to $d$. Let for definiteness $C_{\text{in}} = C_{\text{ex}} = C$, then Eq. (15) can be rewritten as

$$\begin{aligned} \ddot{u}_{p,1} &= \omega_1^2\left(u_{p-1,2} - 2u_{p,1} + u_{p,2}\right) \\ \ddot{u}_{p,2} &= \omega_2^2\left(u_{p,1} - 2u_{p,2} + u_{p+1,1}\right), \end{aligned}$$

where $\omega_1 = \sqrt{\dfrac{C}{M_1}}$, $\omega_2 = \sqrt{\dfrac{C}{M_2}}$. Note that for symmetry reasons, in this case, $d = 2a$.

Next, we introduce the parametrization:

$$M_1 = M\tan\left(\frac{\pi}{4}+\beta\right), \quad M_2 = \frac{M}{\tan(\pi/4+\beta)}, \quad \omega = \sqrt{\frac{C}{M}}$$
$$\omega_1 = \frac{\omega}{\sqrt{\tan(\pi/4+\beta)}}, \quad \omega_2 = \omega\sqrt{\tan\left(\frac{\pi}{4}+\beta\right)}, \quad \frac{\omega_2}{\omega_1} = \tan\left(\frac{\pi}{4}+\beta\right). \tag{16}$$

The parameter $\beta$ can vary from $-\pi/4$ to $\pi/4$. The values $\beta = \pm\pi/4$ correspond to the cases when one of the masses is much larger than the other. It follows from the symmetry of definition (16) that it is sufficient to consider only one half of the interval $\beta \in (-\pi/4; 0)$. For $\omega_1 = \omega_2 = \omega$, that is for $\beta = 0$, we obtain a monatomic chain with a unit cell "length" equal to $a = d/2$.

Let's find the phonon spectrum for one-dimensional diatomic chain [38]. Taking into account the parametrization (16) we have:

$$\Omega_{1,2} = \frac{\Omega^0}{\sqrt{2\cos 2\beta}}\sqrt{1 \pm \sqrt{1-\frac{1}{2}\cos^2 2\beta\Big(1-\cos(Kd)\Big)}}, \tag{17}$$

where $\Omega^0 = 2\omega$ is the maximum frequency value for the corresponding monatomic chain ($\beta = 0$). Note that such a dispersion relation also holds for $C_{\text{in}} \neq C_{\text{ex}}$, $M_1 = M_2 = M$ at the same ratio between frequencies $\dfrac{\omega_2}{\omega_1} = \tan\left(\dfrac{\pi}{4}+\beta\right)$; in this case, $d = 2a$ only for $\beta = 0$.

We find group velocities as the derivative of (17) with respect to the wavenumber

$$c_{g_{1,2}} = \frac{\mathrm{d}\Omega_{1,2}}{\mathrm{d}K} = \mp\,\mathrm{sign}(Kd)\,\frac{c_g^0\Omega^0\cos 2\beta\sin(Kd)}{4\Omega_{1,2}\sqrt{1-\frac{1}{2}\cos^2 2\beta\Big(1-\cos(Kd)\Big)}}, \tag{18}$$

where $c_g^0 = \omega d/2$ is the maximum group velocity for the corresponding monatomic chain ($\beta = 0$).

Figure 2 shows the group velocities for different values of the parameter $\beta$. If $\beta = 0$ we obtain two curves displayed in black for a monatomic chain with a frequency $\omega = \sqrt{C/M}$ and interatomic distance $a = d/2$, the period for which is $\dfrac{2\pi}{a}$ [37]. The curves are shifted relative to each other by $2\pi$; the second curve appears since, in this case, we still solve the system (15) of the two lattice dynamics equations for two neighboring particles.

Let us determine the dependence of the group velocities extrema on $\beta$. The maximum group velocity corresponding to the acoustic branch is obviously $c_{g_2}\Big|_{K=0}$ at any value of $\beta$. The maximum group velocity corresponding to the optic branch is reached in the interval $Kd/2 \in \left(\dfrac{\pi}{2}; \pi\right)$.

The dependence of $c_{g_2}^{\max}$ on $\beta$ is easy to obtain by directing $K$ to zero in formula (18)

$$c_{g_2}^{\max} = c_g^0\sqrt{\cos 2\beta}. \tag{19}$$

We see that for $\beta \in (-\pi/4; 0)$ the maximum group velocity varies from zero to $c_g^0$.

The value $c_{g_1}^{\max}$ for $\beta = 0$ reached at $Kd/2 \to \pi/2$ is of particular interest. In the case of $\beta = 0$, the function $c_{g_1}$ in the interval $Kd/2 \in \left(\dfrac{\pi}{2}; \pi\right)$ yields to

$$c_{g_1}\Big|_{\beta=0} = -\frac{2c_g^0\sin(Kd)}{\sqrt{2+\sqrt{2+2\cos(Kd)}}\sqrt{2+2\cos(Kd)}} \tag{20}$$

and has a discontinuity at point $Kd/2 = \pi/2$. Hence, $c_{g_1}^{\max}$ for $\beta = 0$ is obtained as the limit when $Kd/2$ tends to $\pi/2$ on the right

$$c_{g_1}^{\max}\Big|_{\beta=0} = \lim_{Kd/2\to\pi/2+} c_{g_1}\Big|_{\beta=0} = \frac{c_g^0}{\sqrt{2}} = \frac{1}{\sqrt{2}}c_{g_2}^{\max}\Big|_{\beta=0}. \tag{21}$$

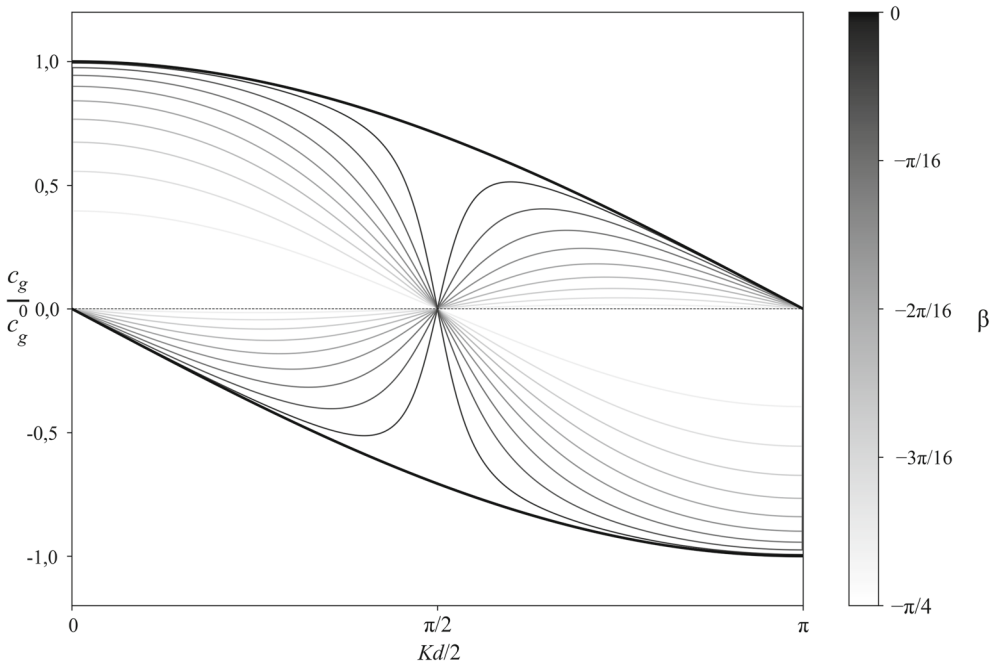


**Fig. 2** Group velocities in a chain of particles with variable masses at various values of $\beta$

Thus, we can conclude that as the masses of particles in a chain become close to each other, the velocity of the heat front corresponding to the optic branch remains finite until exact equality is reached, i.e., two fronts exist apart from each other at a finite distance.

Let us turn to the case $\beta \to -\pi/4$, when one mass is much larger than another. The maximum group velocity corresponding to the acoustic branch behaves as

$$c_{g_2}^{\max} \approx \sqrt{2} c_g^0 \sqrt{\beta + \frac{\pi}{4}} + \mathrm{O}\left(\left(\beta + \frac{\pi}{4}\right)^{5/2}\right). \tag{22}$$

We see that for $\beta \to -\pi/4$ the maximum group velocity corresponding to the acoustic branch decreases as $\sqrt{\beta + \pi/4}$.

The maximum value $c_{g_1}^{\max}$ for $\beta \to -\pi/4$ is reached at $Kd/2 = 3\pi/4$

$$c_{g_1}^{\max}\big|_{Kd/2=3\pi/4} \approx \frac{c_g^0}{\sqrt{2}}\left(\beta + \frac{\pi}{4}\right)^{3/2} + \mathrm{O}\left(\left(\beta + \frac{\pi}{4}\right)^{7/2}\right), \tag{23}$$

so it decreases faster than $c_{g_2}^{\max}$.

Referring to Fig. 2, it is easy to see that the only singular point of the group velocity $c_{g_2}$ (acoustic branch) is $K_* d/2 = 0$. There are two roots of the equation $c'_{g_1} = 0$ in the interval $(\pi/2; \pi)$, and these roots are equal in absolute value. Thus, both singular points related to the optic branch correspond to the same absolute values of $\zeta_*$ and $c''(K_* d)$ [see (9)–(14)], therefore, both intensity coefficients will also be the same.

With these considerations in mind, formula (7) for a diatomic chain can be written as

$$\frac{T}{T_0} \approx \begin{cases} \dfrac{A_1}{\sqrt{\zeta_{1*} - \zeta}} + \dfrac{A_2}{\sqrt{\zeta_{2*} - \zeta}}, & 0 < \zeta < \zeta_{1*} \\ \dfrac{A_2}{\sqrt{\zeta_{2*} - \zeta}}, & \zeta_{1*} < \zeta < \zeta_{2*} \\ 0, & \zeta_{2*} < \zeta \end{cases}, \tag{24}$$

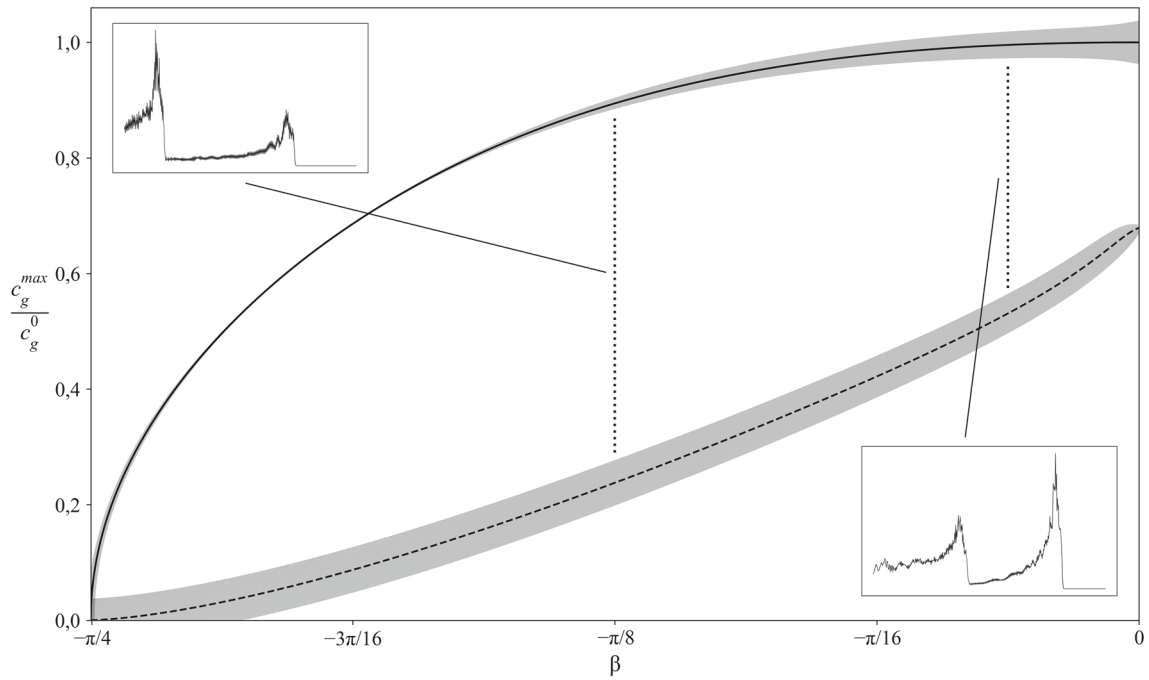


**Fig. 3** Dependence of front propagation velocity on $\beta$ in a chain of particles with variable masses

**Table 1** Velocities and intensity coefficients of thermal wavefronts in extreme cases in a chain of particles with variable masses

| $\beta$ | $-\frac{\pi}{4}$ | 0 |
|---|---|---|
| Acoustic wave speed $\left(c_{g_2}^{\max}\right)$ | $o\left(\sqrt{\beta+\frac{\pi}{4}}\right)$ | $c_g^0$ |
| Acoustic wave intensity coefficient ($a_2$) | 0 | 1 |
| Optic wave speed $\left(c_{g_1}^{\max}\right)$ | $o\left(\left(\beta+\frac{\pi}{4}\right)^{3/2}\right)$ | $\frac{c_g^0}{\sqrt{2}}$ |
| Optic wave intensity coefficient ($a_1$) | 1 | 0 |

where

$$A_1 = \frac{1}{2\pi t\sqrt{2|c''_{g_1}(K_{1*}d)|}}, \quad c'_{g_1}(K_{1*}d) = 0, \quad x_{1*} = |c_{g_1}(K_{1*}d)|$$
$$A_2 = \frac{1}{4\pi t\sqrt{2|c''_{g_2}(K_{2*}d)|}}, \quad c'_{g_2}(K_{2*}d) = 0, \quad x_{2*} = |c_{g_2}(K_{2*}d)| \tag{25}$$

Let us introduce the following notation for the wavefront intensity coefficients

$$a_1 = \frac{A_1}{\sqrt{A_1^2 + A_2^2}}, \quad a_2 = \frac{A_2}{\sqrt{A_1^2 + A_2^2}}, \quad a_1, a_2 \in (0; 1) \tag{26}$$

Figure 3 shows the dependence of front propagation velocities on $\beta$. The thickness of the lines corresponds to the coefficients (26) at the same time $t$. Callouts show the results of a numerical solution for the initial thermal perturbation in the form of a narrow rectangular pulse [31]. Thus, we see that the fundamental solution to the problem of the propagation of thermal perturbations in such a chain always consists of two wavefronts traveling one after another with speeds $c_{g_2}^{\max}$ and $c_{g_1}^{\max}$, respectively.

Let us turn to the limiting cases (see Fig. 3 and Table 1). For $\beta \to -\pi/4$, i.e., one mass is much larger than another, the intensity of the optic front is much higher than the intensity of the acoustic front, whereas the

front propagation velocities are infinitesimal quantities of different orders. This result can be interpreted on another time scale as the main "slow" front, propagating with the speed $c_{g1}^{\max}$, and the "fast" front $c_{g2}^{\max}$ of low intensity. With the increase of $\beta$, the intensity coefficient of the acoustic front increases, and that of the optic front decreases, and when $\beta \approx -\pi/32$, they become equal. In the case when the particle masses differ slightly ($\beta \to 0$), the intensity coefficient of the acoustic front is maximum, and the optic front decays, continuing to travel at nonzero speed.

## 5 Example (ii): A chain with regard for interaction with second neighbors

Next we consider a chain consisting of the equal masses and take into account the interaction with the second neighbors [34].

The equations of lattice dynamics have the form

$$M\ddot{u}_p = C_1\left(u_{p+1} - 2u_p + u_{p-1}\right) + C_2\left(u_{p+2} - 2u_p + u_{p-2}\right), \tag{27}$$

where $u_p$ is the displacement of a particle number $p$, $C_1$ is bond stiffness between neighboring particles, $C_2$ is stiffness of the bond between the particles of the second coordination sphere. Note, that $C_2$ can be both positive and negative.

We introduce the notation,

$$C_0 = C_1 + 4C_2, \tag{28}$$

then the equation of particle dynamics is written as

$$4M\ddot{u}_p = C_0\left(u_{p+2} - 2u_p + u_{p-2}\right) - C_1\left(u_{p+2} - 4u_{p+1} + 6u_p - 4u_{p-1} + u_{p-2}\right) \tag{29}$$

The dispersion relation takes the form

$$\Omega^2 = 4\sin^2\left(\frac{Ka}{2}\right)\left(\omega_0^2\cos^2\left(\frac{Ka}{2}\right) + \omega_1^2\sin^2\left(\frac{Ka}{2}\right)\right), \tag{30}$$

where

$$\omega_0 = \sqrt{\frac{C_1 + 4C_2}{M}}, \quad \omega_1 = \sqrt{\frac{C_1}{M}} \tag{31}$$

Next, we introduce a parametrization similar to (16)

$$\begin{aligned} &\omega_0 = \omega\sqrt{2}\sin\left(\beta + \frac{\pi}{4}\right), \quad \omega_1 = \omega\sqrt{2}\cos\left(\beta + \frac{\pi}{4}\right) \\ &\tan\left(\beta + \frac{\pi}{4}\right) = \frac{\omega_0}{\omega_1} = \sqrt{\frac{C_1 + 4C_2}{C_1}}. \end{aligned} \tag{32}$$

The parameter $\beta$ in this problem also varies from $-\pi/4$ to $\pi/4$, and its sign coincides with the sign of the stiffness $C_2$. For $\beta = 0$ the bond stiffness with the second coordination sphere vanishes, which corresponds to a one-dimensional harmonic chain with the equal masses and stiffnesses. For $\beta = \pi/4$ bond stiffness with the first coordination sphere becomes negligible compared to the stiffness with the second coordination sphere: We obtain a chain with twice the distance between the particles. The value $\beta = -\pi/4$ corresponds to the limiting value of negative stiffness $C_2 = -C_1/4$ for which the chain remains stable.

The dispersion relation finally has the form

$$\Omega = \frac{\Omega^0}{\sqrt{2}}\sqrt{\Big(1 + \sin 2\beta\cos\left(Ka\right)\Big)\Big(1 - \cos\left(Ka\right)\Big)}, \tag{33}$$

and we find the group velocity as the derivative of (33) with respect to the wavenumber

$$c_g = \frac{d\Omega}{dK} = \frac{c_g^0\Omega^0}{2\Omega}\sin\left(Ka\right)\Big(1 + \big(2\cos\left(Ka\right) - 1\big)\sin 2\beta\Big) \tag{34}$$

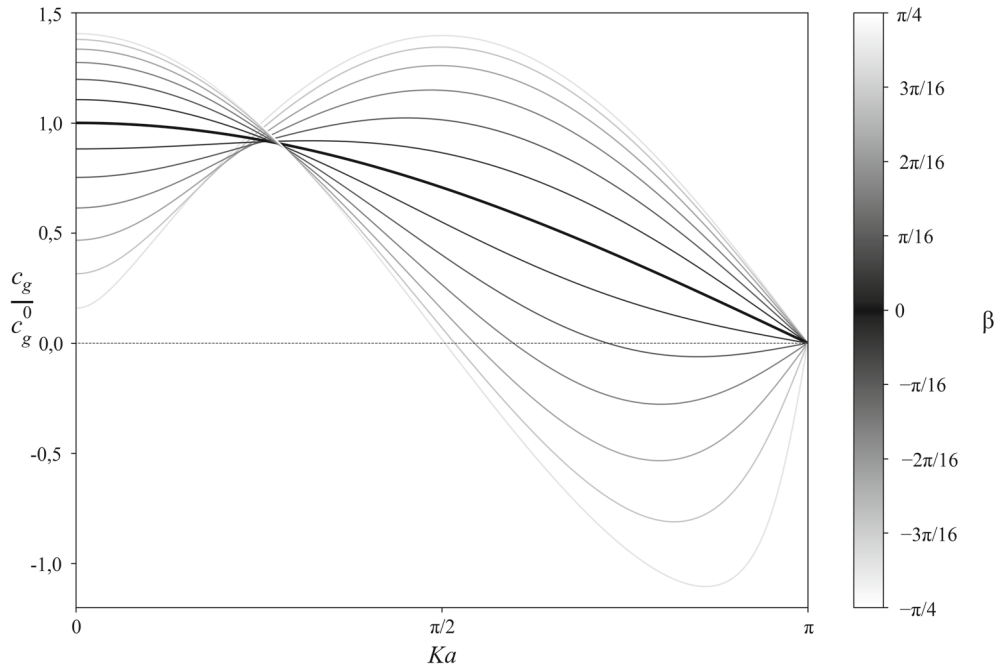


**Fig. 4** Group velocities in a chain with regard for interaction with second neighbors at various values of $\beta$

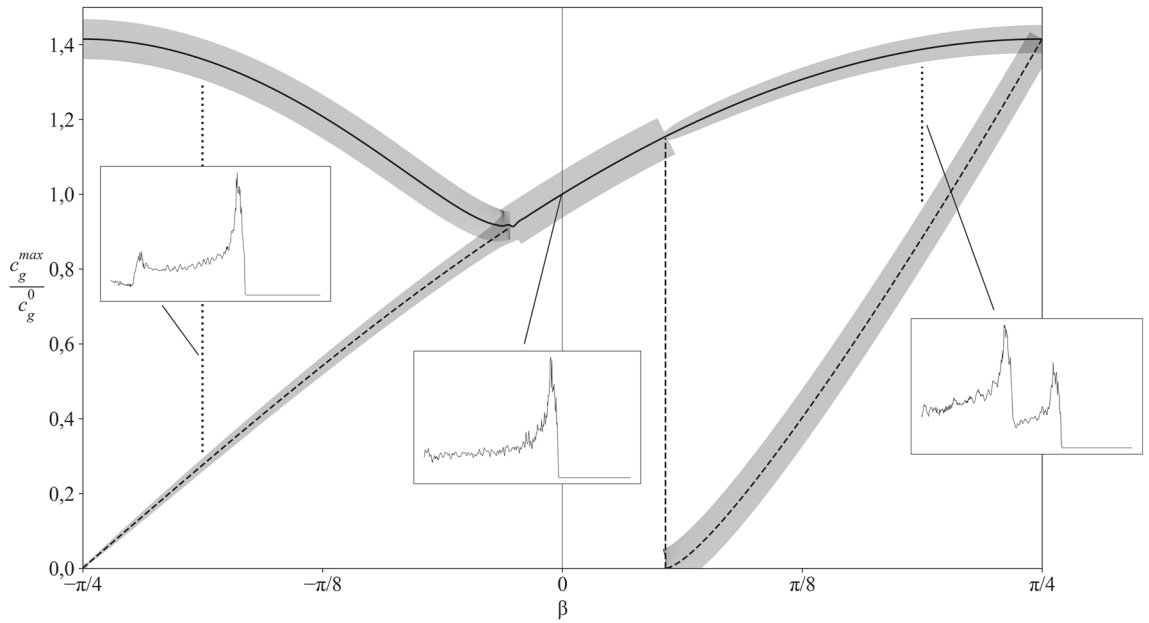


**Fig. 5** Dependence of front propagation velocity on $\beta$ in a chain with regard for interaction with second neighbors

Again, we use the characteristics of a monatomic chain $\Omega^0 = 2\omega$ and $c_g^0 = a\omega$.

Figure 4 shows the group velocities for the considered chain at various values of the parameter $\beta$. If $\beta = 0$ we obtain a curve displayed in black for a monatomic chain with a frequency $\omega_0 = \omega_1 = \omega$ and interatomic distance $a$.

Figure 5 shows the dependence of the extrema of the group velocity on the parameter $\beta$. The solid line corresponds to the maximum propagation velocity of the primary thermal wave, and the dashed line corresponds to that of the second thermal wave. The thickness of the lines corresponds to the coefficients (26) at the same

**Table 2** Velocities and intensity coefficients of thermal wavefronts in extreme cases in a chain with regard for interaction with second neighbors

| $\beta$ | $-\frac{\pi}{4}$ | 0 | $\frac{\pi}{4}$ |
|---|---|---|---|
| Primary wave speed $\left(c_{g_1}^{\max}\right)$ | $\sqrt{2}c_g^0$ | $c_g^0$ | $\sqrt{2}c_g^0$ |
| Primary wave intensity coefficient ($a_1$) | 1 | 1 | $\frac{\sqrt{2}}{2}$ |
| Second wave speed $\left(c_{g_2}^{\max}\right)$ | 0 | – | $\sqrt{2}c_g^0$ |
| Second wave intensity coefficient ($a_2$) | 0 | 0 | $\frac{\sqrt{2}}{2}$ |

time $t$. Callouts show the result of a numerical solution for the initial thermal perturbation in the form of a narrow rectangular pulse [34].

As in the previous section, the fundamental solution of the problem of the propagation of thermal perturbation in the chain, taking into account the second neighbors, consists of two fronts moving one after another with speeds $c_{g_1}^{\max}$ and $c_{g_2}^{\max}$, respectively. In the case of positive $\beta$, the second thermal front arises at a particular value of the parameter with the intensity coefficient exceeding that of the primary wave, but with a lower velocity. For $\beta = \pi/4$, the intensity coefficients and velocities of the two fronts coincide (see Table 2). In the case of negative $\beta$, the second thermal front arises at a certain value of the parameter with the intensity coefficient equal to that of the primary wave. For $\beta = -\pi/4$, both the intensity coefficient and velocity of the second wave go to zero.

## 6 Concluding remarks

This work is devoted to the theoretical basis of prospective practical application of ballistic heat transfer phenomenon. The fact that at the micro-level the heat is carried by thermal waves can be widely used in many areas: from coatings that provide effective heat removal in space systems to signal transmission in NEMS/MEMS. The existing approach [18,26] allows to determine the velocities of these waves, but their intensities are also important. For example, the left callout in Fig. 3 shows a wave that, at certain parameters, travels with a high speed but has such a low intensity that makes it useless in terms of heat transfer, and the main share of energy is carried with a low speed.

In this work, an analytical approach, that bases on the fundamental solution of the heat transfer problem and allows to identify the thermal wavefront intensity, is proposed. Then, the process of heat propagation in the models of (i) a one-dimensional diatomic crystal with variable masses or stiffnesses and (ii) a monoatomic harmonic crystal taking into account interaction with second neighbors is considered. In both cases, we introduce one-dimensionless parameter $\beta \in (-\pi/4; \pi/4)$ the change of which covers the entire class of systems. The value $\beta = 0$ corresponds to a one-dimensional harmonic chain with the equal masses and stiffnesses.

To describe the evolution of the initial thermal perturbation (2), the dispersion characteristics and group velocities are analyzed for the corresponding crystal models. The fundamental solution to the problem of heat propagation in the considered crystals is constructed and analyzed.

In both cases, the solution consists of two fronts moving one after another with different speeds and intensities:

- Problem (i) is symmetric concerning the replacement of $\beta$ to $-\beta$; therefore, the range $\beta \in (-\pi/4; 0)$ is considered. There are always two fronts corresponding to the acoustic and optic branches. With the increase of $\beta$, the intensity coefficient of the acoustic front increases, and that of the optic front decreases, and when $\beta \approx -\pi/32$ they become equal. In the case when the particle masses differ slightly ($\beta \to 0$), the intensity coefficient of the acoustic front is maximum, and the optic front decays, continuing to move at nonzero speed.
- In problem (ii), the system behaves in different ways for positive and negative $\beta$. In the case of positive $\beta$, the second thermal front arises at a particular value of the parameter with an intensity coefficient exceeding that of the primary wave, but with a slower speed. For $\beta = \pi/4$, intensity coefficients and velocities of two fronts coincide. In the case of negative $\beta$, the second thermal front arises at a certain value of the parameter

with the intensity coefficient equal to that of the primary wave. For $\beta = -\pi/4$, both the intensity coefficient and velocity of the second wave go to zero.

Thus, two mechanisms of the evolution of the thermal wavefronts in one-dimensional systems are revealed. The results can be used to extract those parts of the wave processes that are of interest in terms of interpretation of the effects observed in the experiments.

**Acknowledgements** The authors are deeply grateful to Dr. V.A. Kuzkin and Prof. A.V. Porubov for useful discussions.

**Note added in proof** The article was translated from Russian with the permission of the respective journal: Loboda, O.S., Podolskaya, E.A., Tsvetkov, D.V., Krivtsov, A.M.: On the fundamental solution of the heat transfer problem in one-dimensional harmonic crystals. Comput. Cont. Mech., 12(4), 390–402 (2019). https://doi.org/10.7242/1999-6691/2019.12.4.33.

## References

1. Peierls, R.E.: Quantum Theory of Solids. Clarendon Press, Oxford (1965)
2. Ziman, J.M.: Electrons and Phonons: The Theory of Transport Phenomena in Solids. Oxford University Press, New York (1960)
3. Askar, A.: Lattice Dynamical Foundations of Continuum Theories. Word Scientific, Singapore (1985)
4. Maugin, G.A.: Nonlinear Waves in Elastic Crystals. Oxford University Press, New York (1999)
5. Askes, H., Metrikine, A.V.: Higher-order continua derived from discrete media: continualisation aspects and boundary conditions. Int. J. Solids Struct. **42**, 187–202 (2005). https://doi.org/10.1016/j.ijsolstr.2004.04.005
6. Indeitsev, D.A., Sergeev, A.D.: Correlation between the properties of eigenfrequencies and eigenmodes in a chain of rigid bodies with torque connections. Vestn. St. Petersb. Univ. Math. **50**, 166–172 (2017). https://doi.org/10.3103/S1063454117020066
7. Morozov, N.F., Muratikov, K.L., Semenov, B.N., Indeitsev, D.A., Vavilov, D.S.: Thermoacoustics of conductive materials under laser action. Dokl. Phys. **64**, 169–172 (2019). https://doi.org/10.1134/S1028335819040037
8. Metrikine, A.V., Askes, H.: An isotropic dynamically consistent gradient elasticity model derived from a 2D lattice. Philos. Mag. **86**, 3259–3286 (2006). https://doi.org/10.1080/14786430500197827
9. Potapov, A.I., Pavlov, I.S., Gorshkov, K.A., Maugin, G.A.: Nonlinear interactions of solitary waves in a 2D lattice. Wave Motion **34**, 83–96 (2001). https://doi.org/10.1016/S0165-2125(01)00061-0
10. Pavlov, I.S., Potapov, A.I., Maugin, G.A.: A 2D granular medium with rotating particles. Int. J. Solids Struct. **43**, 6194–6207 (2006). https://doi.org/10.1016/j.ijsolstr.2005.06.012
11. Golovnev, I.F., Golovneva, E.I., Fomin, V.M.: Investigation of thermal instability in nano-dimensional systems by molecular dynamics method. AIP Conf. Proc. **2027**, 030143 (2018). https://doi.org/10.1063/1.5065237
12. Vasiliev, A.A., Dmitriev, S.V., Miroshnichenko, A.E.: Multi-field continuum theory for medium with microscopic rotations. Int. J. Solids Struct. **42**, 6245–6260 (2005). https://doi.org/10.1016/j.ijsolstr.2005.03.0411
13. Vasiliev, A.A., Dmitriev, S.V., Miroshnichenko, A.E.: Multi-field approach in mechanics of structured solids. Int. J. Solids Struct. **47**, 510–525 (2010). https://doi.org/10.1016/j.ijsolstr.2009.10.016
14. Le-Zakharov, A.A., Krivtsov, A.M.: Molecular dynamics investigation of heat conduction in crystals with defects. Dokl. Phys. **53**, 261–264 (2008). https://doi.org/10.1134/S1028335808050066
15. Chandrasekharaiah, D.S.: Thermoelasticity with second sound: a review. Appl. Mech. Rev. **39**, 355–376 (1986). https://doi.org/10.1115/1.3143705
16. Poletkin, K.V., Gurzadyan, G.G., Shang, J., Kulish, V.: Ultrafast heat transfer on nanoscale in thin gold films. Appl. Phys. B **107**, 137–143 (2012). https://doi.org/10.1007/s00340-011-4862-z
17. Rieder, Z., Lebowitz, J.L., Lieb, E.: Properties of a harmonic crystal in a stationary nonequilibrium state. J. Math. Phys. **8**, 1073–1078 (1967). https://doi.org/10.1063/1.1705319
18. Kuzkin, V.A., Krivtsov, A.M.: Fast and slow thermal processes in harmonic scalar lattices. J. Phys.: Condens. Matter. **29**, 505401 (2017). https://doi.org/10.1088/1361-648X/aa98eb
19. Dhar, A.: Heat transport in low-dimensional systems. Adv. Phys. **57**, 457–537 (2008). https://doi.org/10.1080/00018730802538522
20. Lepri, S. (ed.): Thermal Transport in Low Dimensions: From Statistical Physics to Nanoscale Heat Transfer. Springer, Switzerland (2016)
21. Guzev, M.A.: The Fourier's law for a one-dimensional crystal. Dalnevost. Mat. Zh. **18**(1), 34–38 (2018)
22. Sokolov, A.A., Krivtsov, A.M., Müller, W.H.: Localized heat perturbation in harmonic 1D crystals: solutions for the equation of anomalous heat conduction. Phys. Mesomech. **20**, 305–310 (2017). https://doi.org/10.1134/S1029959917030067
23. Kuzkin, V.A., Krivtsov, A.M.: High-frequency thermal processes in harmonic crystals. Dokl. Phys. **62**, 85–89 (2017). https://doi.org/10.1134/S1028335817020070
24. Kuzkin, V.A., Krivtsov, A.M.: An analytical description of transient thermal processes in harmonic crystals. Phys. Solid State **59**, 1051–1062 (2017). https://doi.org/10.1134/S1063783417050201
25. Krivtsov, A.M.: Energy oscillations in a one-dimensional crystal. Dokl. Phys. **59**, 427–430 (2014). https://doi.org/10.1134/S1028335814090080
26. Krivtsov, A.M.: Heat transfer in infinite harmonic one-dimensional crystals. Dokl. Phys. **60**, 407–411 (2015). https://doi.org/10.1134/S1028335815090062
27. Krivtsov, A.M.: The ballistic heat equation for a one-dimensional harmonic crystal. In: Altenbach, H., Belyaev, A., Eremeyev, V., Krivtsov, A., Porubov, A. (eds.) Dynamical Processes in Generalized Continua and Structures, pp. 345–358. Springer, Berlin (2019). https://doi.org/10.1007/978-3-030-11665-1_19

28. Gavrilov, S.N., Krivtsov, A.M.: Thermal equilibration in a one-dimensional damped harmonic crystal. Phys. Rev. E **100**, 022117 (2019). https://doi.org/10.1103/PhysRevE.100.022117
29. Berinskii, I.E., Kuzkin, V.A.: Equilibration of energies in a two-dimensional harmonic graphene lattice. Philos. Trans. Math. Phys. Eng. Sci. **378**, 20190114 (2019). https://doi.org/10.1098/rsta.2019.0114
30. Kosevich, A.M., Savotchenko, S.E.: Peculiarities of dynamics of one-dimensional discrete systems with interaction extending beyond nearest neighbors and the role of higher dispersion in soliton dynamics. Low Temp. Phys. **25**, 550–557 (1999). https://doi.org/10.1063/1.593783
31. Michelitsch, T.M., Collet, B., Wang, X.: Nonlocal constitutive laws generated by matrix functions: lattice dynamics models and their continuum limits. Int. J. Eng. Sci. **80**, 106–123 (2014). https://doi.org/10.1016/j.ijengsci.2014.02.029
32. Porubov, A.V., Krivtsov, A.M., Osokina, A.E.: Two-dimensional waves in extended square lattice. Int. J. Non-Linear Mech. **99**, 281–287 (2018). https://doi.org/10.1016/j.ijnonlinmec.2017.12.008
33. Podolskaya, E.A., Krivtsov, A.M., Tsvetkov, D.V.: Anomalous heat transfer in one-dimensional diatomic harmonic crystal. Mater. Phys. Mech. **40**, 172–180 (2018). https://doi.org/10.18720/MPM.4022018_5
34. Loboda, O., Krivtsov, A., Porubov, A., Tsvetkov, D.: Thermal processes in a one-dimensional crystal with regard for the second coordination sphere. ZAMM **99**, e201900008 (2019). https://doi.org/10.1002/zamm.201900008
35. Kuzkin, V.A.: Thermal equilibration in infinite harmonic crystals. Cont. Mech. Thermodyn. **31**, 401–423 (2019). https://doi.org/10.1007/s00161-019-00758-2
36. Gelfand, I.M., Shilov, G.E.: Generalized Functions. Vol. 1: Properties and Operations. AMS Chelsea Publishing, New York (1964)
37. Ashcroft, N., Mermin, N.: Solid State Physics. Saunders College Publishing, Philadelphia (1976)
38. Mandelshtam, L.I.: Complete Works. Vol. IV: Lectures on Oscillations. Publishing House of the Academy of Sciences of the USSR, Moscow (1955)